Pergamon

Neuropharmacology 39 (2000) 1–10

NEURO PHARMACOLOGY

www.elsevier.com/locate/neuropharm

Determinants of voltage-dependent inactivation affect Mibefradil block of calcium channels

Cristina Jiménez [a], Emmanuel Bourinet [a], Valérie Leuranguer [a], Sylvain Richard [a], Terry P. Snutch [b], Joël Nargeot [a,*]

[a] *Institut de Génétique Humaine, CNRS UPR1142, 141 Rue de la Cardonille, 34396 Montpellier, cedex 5, France*
[b] *Biotechnology Laboratory, Rm.237, University of British Columbia Westbrook Bldg., Vancouver BC, V6T 1Z3, Canada*

Accepted 27 July 1999

Abstract

The voltage gated calcium channel family is a major target for a range of therapeutic drugs. Mibefradil (Ro 40–5967) belongs to a new chemical class of these molecules which differs from other Ca^{2+} antagonists by its ability to potently block T-type Ca^{2+} channels. However, this molecule has also been shown to inhibit other Ca^{2+} channel subtypes. To further analyze the mechanism governing the Ca^{2+} channel–Mibefradil interaction, we examined the effect of Mibefradil on various recombinant Ca^{2+} channels expressed in mammalian cells from their cloned cDNAs, using Ca^{2+} as the permeant ion at physiological concentration. Expression of α_{1A}, α_{1C} and α_{1E} in tsA 201 cells resulted in Ca^{2+} currents with functional characteristics closely related to those of their native counterparts. Mibefradil blocked α_{1A} and α_{1E} with a Kd comparable to that reported for T-type channels, but had a lower affinity (~30-fold) for α_{1C}. For each channel, inhibition by Mibefradil was consistent with high-affinity binding to the inactivated state. Modulation of the voltage-dependent inactivation properties by the nature of the coexpressed β subunit or the α1 splice variant altered block at the Mibefradil receptor site. Therefore, we conclude that the tissue and sub-cellular localization of calcium channel subunits as well as their specific associations are essential parameters to understand the in vivo effects of Mibefradil.

Keywords: Calcium antagonist; State-dependent block; Ancillary subunits; Modulated receptor hypothesis; Recombinant calcium channels; Human embryonic kidney cells

1. Introduction

Voltage-gated calcium channels (VGCCs), are transmembrane proteins involved in the regulation of cellular excitability and Ca^{2+} homeostasis. VGCCs, classified as L-, N-, P-, Q-, R- and T-type based on their functional properties, are critical for many cellular functions including muscular contraction, neurotransmitter release and excitability. To date, ten Ca^{2+} channels genes have been reported and termed α_{1S} for the first one identified in skeletal muscle and α_{1A} through to α_{1I} for the nine others isolated subsequently (Perez-Reyes et al., 1998). When transiently expressed from their cDNA in a host system together with their ancillary β and $\alpha_2\delta$ subunits, α_{1A} exhibits the characteristics of P- and Q-type channels, α_{1B} encodes an N-type channel, α_{1C} α_{1D} and α_{1S} constitute three different types of L-type channels, and α_{1E} seems to correlate to resistant R-type channels defined as VGCCs insensitive to all known Ca channel antagonists and toxins. The recently described α_{1F} gene is highly homologous to α_{1D} and probably corresponds to an L-type channel (Fisher et al., 1997). Finally, α_{1G} α_{1H} and α_{1I} the latest genes identified, have been unambiguously characterized as members of the T-type Ca channel family (Perez-Reyes et al., 1998; Cribbs et al., 1998; Lee et al., 1999).

VGCCs are major targets for a variety of therapeutic agents such as dihydropyridines (DHPs), benzothiazepines (BTZs), and phenylalkylamines (PPAs) that are used in the treatment of hypertension, stroke, acute ischemia, migraine and epilepsy. These drugs are considered as L-

* Corresponding author. Tel.: +33-499-619967; fax: +33-499-619901.
E-mail address: joel.nargeot@igh.cnrs.fr (J. Nargeot)

0028-3908/00/$ - see front matter
PII: S0028-3908(99)00153-7

type Ca^{2+} channel antagonists. In addition to the DHPs, BTZs and PAAs, a new molecule (Mibefradil, a tetralole derivative) has been described with a potent action on low-voltage activated T-type VGCCs (Mishra and Hermsmeyer, 1994). Mibefradil has proven to be effective in the treatment of cardiovascular diseases but the relationship between the clinical effect (hypotension with no increase in heart rate) and the inhibition of T-type channels has not clearly been established. In addition to the block of T-type Ca^{2+} channels, Mibefradil was also reported to block channels induced by α_{1A}, α_{1B}, α_{1C} and α_{1E} expression in *Xenopus* oocytes (Bezprozvanny and Tsien, 1995). To further compare Mibefradil blockade of different calcium channel subtypes, we studied its action on three major classes of cloned Ca^{2+} channels. Our results provide the first comparison of the effect of Mibefradil on recombinant α_{1A}, α_{1C}, α_{1E} currents in nearly physiological conditions (transiently expressed in mammalian cells and currents recorded in physiological levels of external calcium). In addition, our results show that the voltage-dependent kinetics of inactivation of Ca^{2+} channels, determined by the nature of the associated β subunit isoform and/or alternative splicing of the $\alpha 1$ gene, is critical for the action of Mibefradil.

2. Materials and methods

2.1. Transient expression of recombinant calcium channels

cDNAs encoding VGCCs α_1, α_2 and β subunits and reporter genes (CD8 or GFP) were inserted in vertebrate expression vectors. Rat brain α_{1A} isoforms, α_{1E}, β_{2a}, and $\alpha_2\delta$ were cloned in pMT2 (Stea et al., 1994; Soong et al., 1993; Bourinet et al., 1999); rat brain α_{1C} and β_{1b}, in pCEP4 (Tomlinson et al., 1993); and CD8 (generously provided by Dr Brian Seed, Massachusetts General Hospital) and GFP (a kind gift from Dr Kye Chesnut, University of Florida) in CMV promoter driven vectors. Human embryonic kidney cells expressing the SV40 large antigen (tsA201 cells) were obtained from Dr Richard Horn (Jefferson Medical College). They were grown in DMEM medium supplemented with 10% fetal bovine serum and 1% penicillin/streptomycin (v/v). For optimal transfection, cells were plated at 30–40% confluence on glass coverslips coated with poly-L-ornithine. A calcium phosphate transfection procedure was used with an α_1-$\alpha_2\delta$-β-CD8 or GFP cDNA mix at a molar ration of 1:1:1:0.1. After an incubation of at least 48 hours, positively transfected cells were identified either with anti-CD8 antibody coated beads (when CD8 was cotransfected), or using an epifluorescence illumination source on the microscope (when GFP was cotransfected). For *Xenopus* oocyte transient expression, stage V and VI oocytes were prepared as described (Bourinet et al., 1996), and nuclear injection was performed with 10 nl of an α_1-$\alpha_2\delta$-β cDNA mix (1:1:1 molar ratio). Oocytes were then incubated at 18°C for three to six days in ND96 medium.

2.2. Electrophysiology

Positively transfected tsA201 cells were analyzed by whole-cell patch clamp using either a Biologic RK300 or an Axopatch 200A amplifier. Leak and capacitive currents were subtracted using a P/5 method. Except where indicated in the text, currents were evoked with 50 ms long depolarizing pulses from −100 mV to the potential giving the maximum inward current delivered at 0.1 Hz. Extracellular solution contained (in mM): 2 $CaCl_2$, 160 TEACl, 10 HEPES (pH to 7.4 with TEAOH). Pipettes of typical resistance of 1–2 MΩ, made of borosilicate glass, were filled with an internal solution containing (in mM): 110 CsCl, 3 $MgCl_2$, 10 EGTA, 10 HEPES, 3 Mg-ATP, 0.6 GTP (pH to 7.2 with CsOH). Mibefradil (a gift from Dr Robert Koen, Produits Roche) was prepared daily in the external solution at 10 mM. The various dilutions were applied to cells by gravity driven perfusion controlled by solenoid valves.

Macroscopic oocyte currents were recorded using two electrode voltage-clamp as described (Bourinet et al., 1996) in a solution containing (in mM): 5 $BaOH_2$, 25 TEAOH, 25 NaOH, 2 CsOH, 30 NMDG, 5 HEPES (pH to 7.3 with methanesulfonic acid). The endogenous oocyte Ca^{2+}-activated Cl^- current was completely suppressed by injection of a BAPTA solution (2–5 mM estimated final concentration). On line leak subtracted currents were evoked at 0.1 Hz by 100 ms long depolarizing pulses from −80 to 0 mV. Oocytes were continuously perfused and Mibefradil dilutions were applied by a perfusion system controlled by solenoid valves.

pClamp6 software was used for data acquisition and analysis. Current-voltage curves were fitted using a modified Boltzmann equation as described (Bourinet et al., 1996). Inactivation curves were constructed by normalizing the current after a 15 sec conditioning prepulse and then fitted to a Boltzmann equation. Apparent dissociation constants (Kd) were obtained from the fits of the Mibefradil dose-response curves using a sigmoidal function. Results are presented as the mean±SEM.

3. Results

3.1. Recombinant Ca^{2+} currents in mammalian cells

Transfection of rat α_{1A}, α_{1C}, or α_{1E} with α_2-δ and β_{1b} subunits produced a robust expression of Ca^{2+} channels as determined by the presence of a large Ca^{2+} current density. This allowed the comparison of these three major

types of VGCCs with a physiological concentration of Ca^{2+} as the charge carrier. The α_{1A} α_{1C} and α_{1E} channels were activated by depolarization greater than −40 to −30 mV, had a maximum amplitude around 0 mV, and reversed near +60 mV (Fig. 1). They all deactivated with monoexponential decay kinetics which was best fitted with a time constant of less than 1 ms (in the range of 0.2 to 0.5 ms, data not shown). As expected from previous work (DeLeon et al., 1995; Bourinet et al., 1996), comparison of current kinetics using either Ca^{2+} or Ba^{2+} as the charge carrier showed that, unlike α_{1A} and α_{1E}, the recombinant α_{1C} L-type currents displayed marked Ca^{2+}-dependent inactivation comparable to that observed for native L-type currents (data not shown).

3.2. Dose-dependence of Mibefradil block

We studied the antagonistic effect of Mibefradil on the Ca^{2+} currents generated by α_{1A}, α_{1C}, and α_{1E}. The dose-response curves in Fig. 2A show that the α_{1A} and α_{1E} channels were blocked in the sub-micromolar concentration range (apparent Kd of 0.3 and 0.4 μM respectively), while at least a 10 fold higher concentration was required to produce an equivalent block of the α_{lC} channels (apparent Kd of 12 μM). All three dose-response curves were best fitted with a Hill number of 1; consistent with a 1 to 1 Mibefradil to Ca^{2+} channel interaction. Comparison of the current traces obtained before and after the steady state effect of 1 μM Mibefradil is reached, further illustrates this difference in sensitivity (Fig. 2B). More than 75% of the α_{1A} and α_{1E} currents were blocked while the α_{1C} current was almost unaffected.

3.3. Voltage-dependent block

Mibefradil block of all high-voltage-activated Ca^{2+} channel subtypes has previously been suggested to be strongly dependent on the resting membrane potential (Bezprozvanny and Tsien, 1995; but see also Aczél et al., 1998). Therefore, we tested whether or not this also occurred in our experimental conditions. Ca^{2+} currents were evoked from a holding potential (HP) of either −100 mV or −60 mV. Fig. 3 shows the significant leftward shift in the dose response-curves without modification of the slope observed when the HP was switched

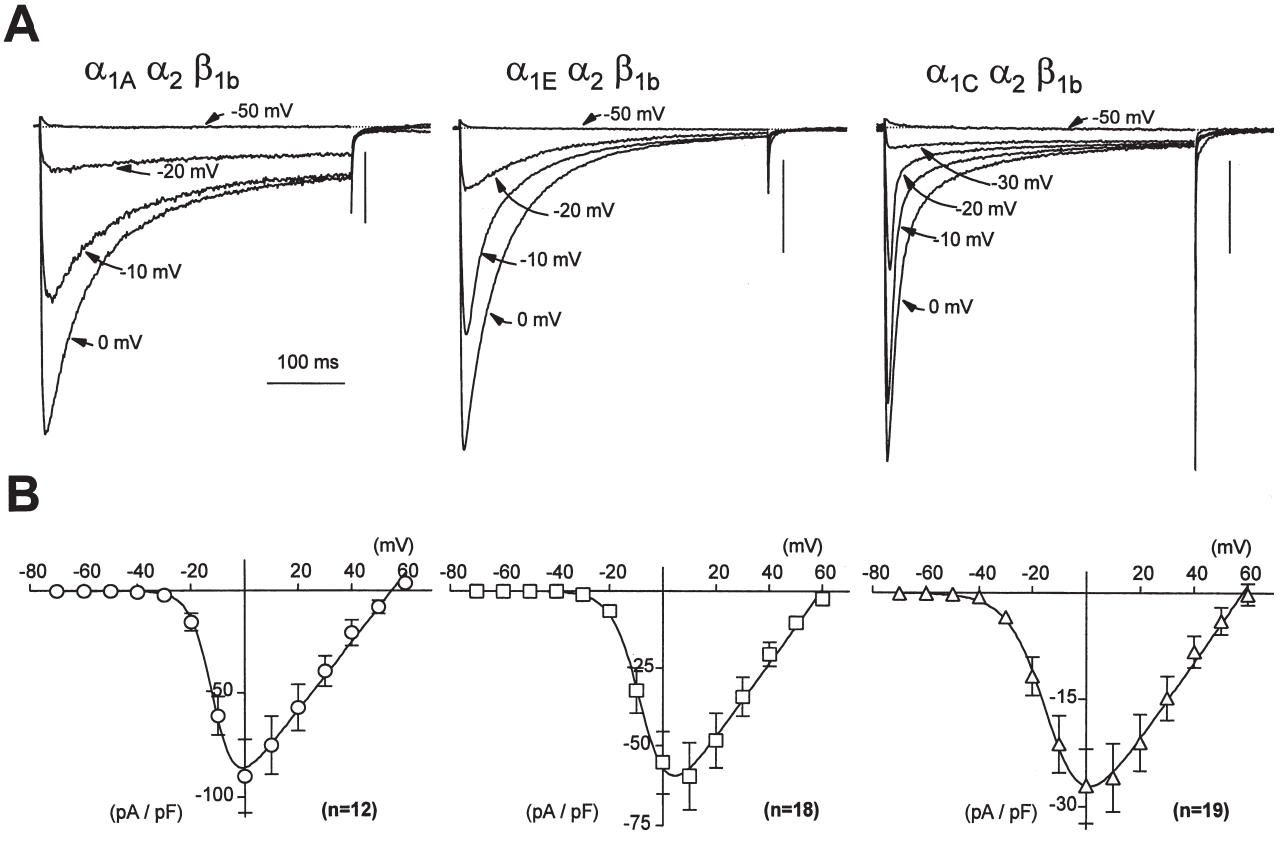

Fig. 1. Calcium current characteristics of recombinant calcium channels in HEK cells. (A) Representative whole-cell Ca^{2+} current generated by the three different channels. Currents were elicited by 400 ms step depolarizations to the indicated potentials from a holding potential of −100 mV. Scale bar amplitudes correspond respectively to 0.5 nA (α_{1A}), 1 nA (α_{1E}), and 0.4 nA (α_{1C}). (B) Plot of the mean current density-voltage relationship corresponding to the channel types shown in (A). The thick line across the data points correspond to the best fit using a modified Boltzmann equation. The deduced values for half activation (Vh) and slope of activation (k) are respectively (in mV): −11.2 and −4.2 (α_{1A}); −7.4 and −5.1 (α_{1E}); −12.3 and −7.3 (α_{1C}).

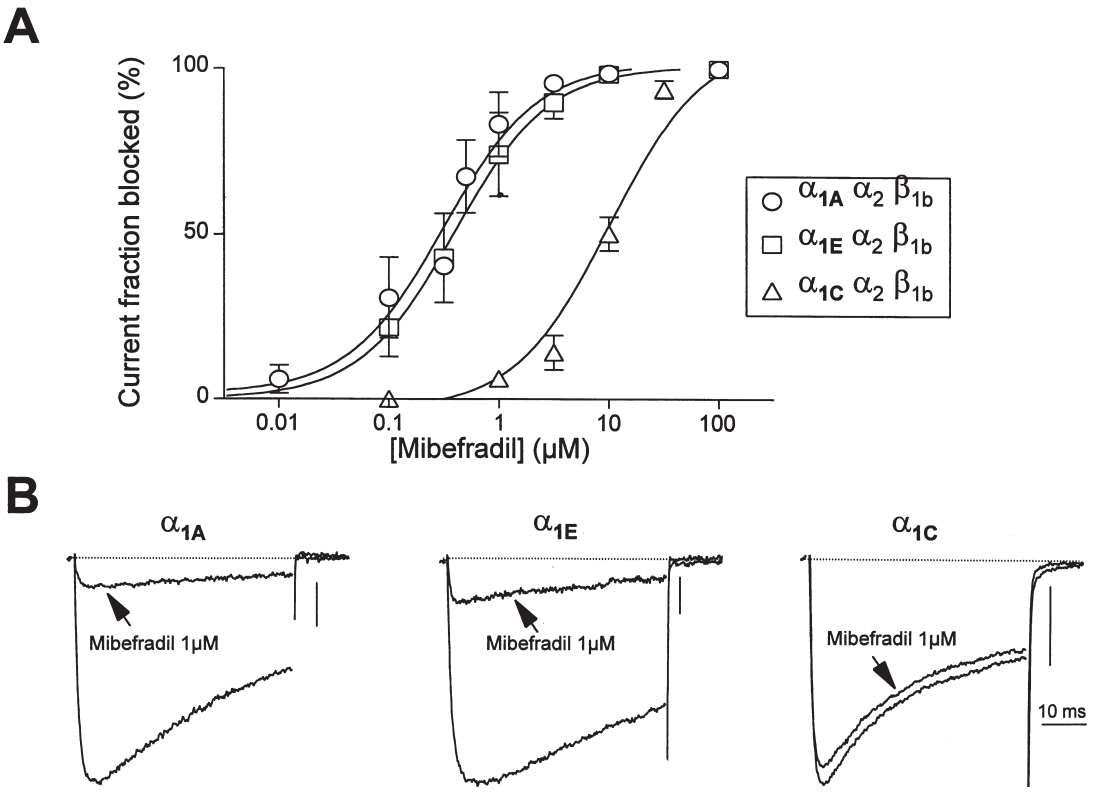

Fig. 2. Block of whole cell current by Mibefradil. (A) Dose-response curves for Mibefradil block (open circles: α_{1A} α_2 β_{1b}; open square: α_{1E} α_2 β_{1b}; open triangle: α_{1C} α_2 β_{1b}). The results indicates that α_{1A} and α_{1E} channels are more potently blocked than α_{1C}. The data are well described by a Hill coefficient of 1, suggesting a 1:1 interaction between the channel and the drug. (B) Representative current traces before and after the application of 1 μM Mibefradil. Currents were evoked by 50 ms step depolarizations from −100 mV to 0 mV at 0.1 Hz. Scale bars beside the current traces correspond to 0.3 nA.

from −100 to −60 mV. Mibefradil was 4 to 5 fold more potent when the membrane was maintained at the less polarized potential. Apparent Kds at −100 mV and −60 mV were respectively 0.3 μM and 0.06 μM for α_{1A}, 0.4 μM and 0.02 μM for α_{1E}, and 12 μM and 3 μM for α_{1C}. Consistent with these findings we observed a significant leftward shift (7 mV) of the α_{1A} inactivation curve in the presence of 1 μM Mibefradil ($V_{0.5}$ cont: −39 mV; $V_{0.5}$ Mib: −46 mV). Furthermore, the rate of drug washout (Koff) was dramatically speeded up at hyperpolarized potentials (data not shown). These data are consistent with a preferential effect of Mibefradil on the inactivated state of each Ca^{2+} channel subtype (Bezprozvanny and Tsien, 1995).

3.4. Modulation by β-subunits

We further assessed whether factors influencing the voltage-dependent inactivation of α_{1A}, α_{1E} and α_{1C} modulate the effect of Mibefradil. In particular, we concentrated our study on the potential role of the various β subunits, in view of their differential modulation of the decay kinetics of Ca^{2+} currents. For example, the β_2 isoform promotes a slowing of the voltage-dependent inactivation of the Ca^{2+} current generated by most of the α1 subtypes (Olcese et al., 1994; Qin et al., 1998). Similar results are reported on Fig. 4 which shows that the global decay kinetics of the Ca^{2+} currents generated by α_{1A}, α_{1E} and α_{1C} were much slower when coexpressed with β_{2a} instead of β_{1b} (Fig. 4A). Consistent with the slower kinetics, the steady-state inactivation curves of α_{1A} and α_{1E} were dramatically shifted towards a more positive potential in the presence of β_{2a} (Fig. 4B). In contrast, almost no shift was observed with α_{1C} but the inactivation time course was incomplete (Fig. 4B) consistent with the presence of the non-inactivating component observed in Fig. 4A. Therefore the effect of Mibefradil would be predicted to be dependent upon the nature of the β-subunit.

The effect of Mibefradil was therefore compared in the presence of either the β_{1b} or the β_{2a} subunit. First, it was obvious that the inhibition of each type of current (i.e. currents generated by α_{1A}, α_{1E} and α_{1C}) was weaker with β_{2a} (Fig. 5). The concentration of drug required to block the same fraction of current was approximately 10 fold higher for α_{1A} (Kd[β_{1b}] 0.3 μM; Kd[β_{2a}] 3 μM) and for α_{1E} (Kd[β_{1b}] 0.4 μM; Kd(β_{2a}) 3 μM). There was much less difference in the case of α_{1C} (Kd[β_{1b}] 12 μM ; Kd[β_{2a}] 21 μM) probably due to the smaller effect of β_{2a} on the steady-state inactivation curve of α_{1C} (Fig. 4B).

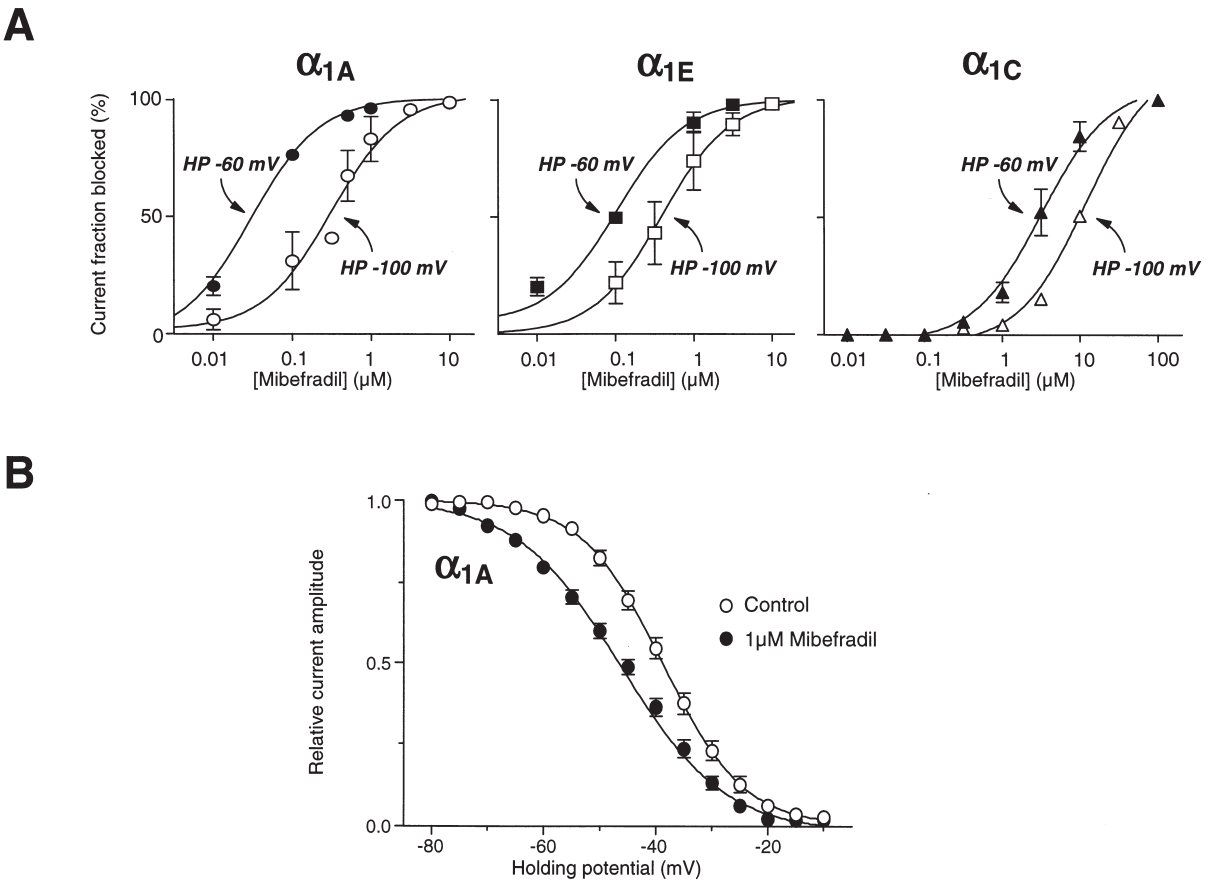

Fig. 3. Increase in Mibefradil block by depolarized holding potential. (A) Comparison of dose-responses of Mibefradil block of α_{1A}, α_{1E} or α_{1C} ($+\alpha_2$ and β_{1b}) at holding potentials of −100 mV and −60 mV respectively. Note that depolarization increased substantially channel sensitivity towards the drug. Step depolarizations of 50 ms to 0 mV were delivered either from −100 mV or −60 mV at 0.1 Hz. (B) Effect of 1 μM Mibefradil on the steady-state inactivation curve of α_{1A} ($+\alpha_2$ and β_{1b}). Note the significant shift of the curve to the left in the presence of the drug. A 5 sec conditioning depolarization and a 100 ms test pulse were applied every 25 s (interval sufficient to allow recovery from inactivation).

3.5. Differential block of α_1 splice variants

In addition to the differential modulatory effects of the β subunit isoforms, each α_1 subunit also exhibits distinct biophysical properties. Certain critical regions within the α_1 molecules determining their diverse voltage-dependent inactivation have been mapped by structure-function studies (Zhang et al., 1994; Parent et al., 1995). It was notably shown that an alternatively spliced α_{1A} isoform (α_{1A-b}) exhibits markedly reduced inactivation (Bourinet et al., 1999). This effect was attributed to a single amino acid insertion within the linker between the first and the second transmembrane domain. Thus, we compared the Mibefradil block of α_{1A-b} and α_{1A-a}. As it was difficult to obtain comparable current densities of these isoforms in tsA201 cells, we transiently expressed them in *Xenopus* oocytes, where they generate similar current density. Inactivation protocols showed the distinct inactivation of the two α_{1A} variants. While the α_{1A-a} current was almost totally inactivated at the end of a 15 s depolarization to 0 mV, a large component of α_{1A-b} current remained (~20% inactivated current Fig. 6A). Construction of the inactivation curves from these protocols further indicated partial inactivation of α_{1A-b} channels and a shift by about 20 mV towards more depolarized potentials. When HPs were maintained for at least one minute to achieve steady-state conditions (see protocol in Fig. 6B), the fraction of current inactivated at −80 mV was negligible for α_{1A-b} but substantial for α_{1A-a} channels (Fig. 6B). In parallel with these differences in inactivation properties, the dose-response curves (Fig. 6C) showed that α_{1A-b} was much less sensitive to Mibefradil than α_{1A-a} (Kd [α_{1A-a}]=12 μM vs Kd [α_{1A-b}]=66 μM).

3.6. Use dependent inhibition

In addition to the voltage-dependent block, some calcium antagonists decrease Ca^{2+} channel activity with a use-dependent effect. In this process drug action is conditioned by repetitive opening of the channel. This type of block is enhanced upon increasing the stimulation frequency. Bezprozvanny and Tsien (1995) as well as Aczél et al. (1998) have demonstrated the use-dependent effect

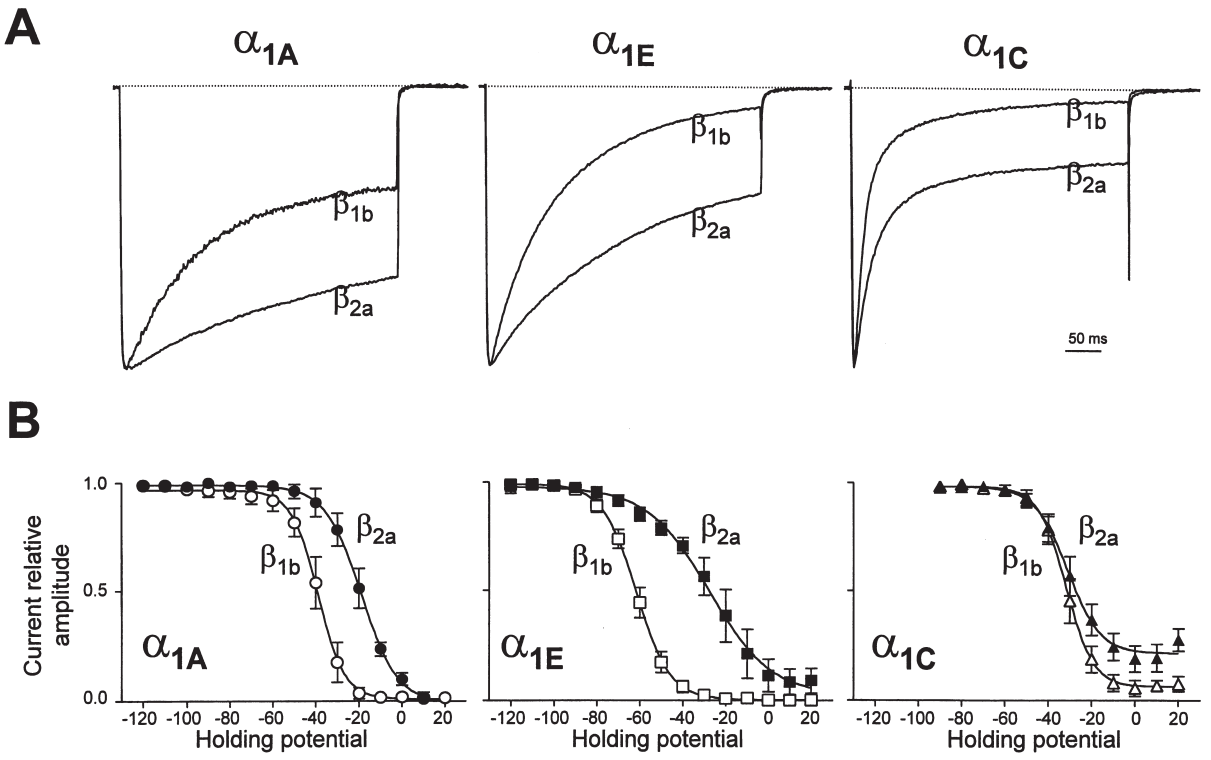

Fig. 4. Comparison of the voltage-dependent inactivation of recombinant Ca^{2+} channels with two distinct β subunits. (A) Inactivation kinetics of all Ca^{2+} channels are slowed by β_{2a} subunit coexpression. (B) Mean steady state inactivation curves obtained for 8 to 15 cells with either β_{1b} or β_{2a} subunits. Boltzmann fit across the data point clearly show that β_{2a} shifted the curve toward more depolarized potentials for α_{1A} and α_{1E}, while α_{1C} is less affected.

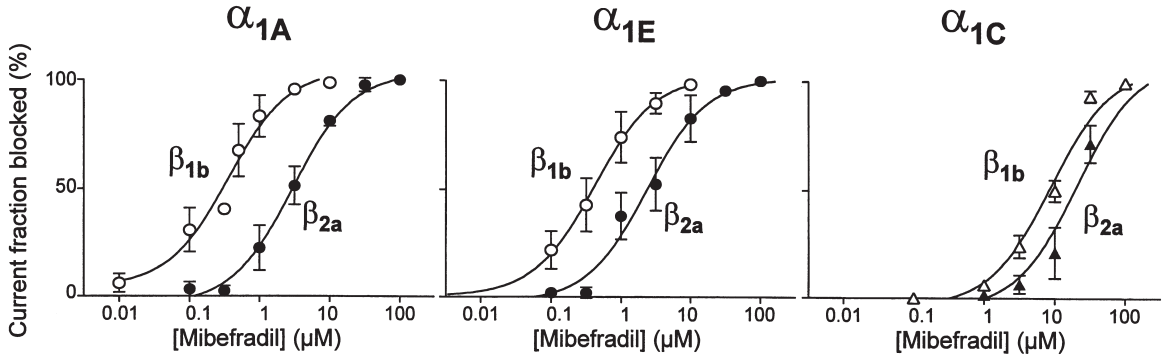

Fig. 5. Coexpression of Ca^{2+} channel with β_{2a} results in a reduced blocking efficacy by Mibefradil. Dose-response curves obtained with α_{1A}, α_{1E}, and α_{1C} coexpressed with α_2 and with either β_{1b} or β_{2a}. The stimulation protocol was as described in Fig. 2. Note that the magnitude of the β_{2a} effect on Mibefradil block parallels the β_{2a} modulation of the steady state inactivation shown in Fig. 4B.

of Mibefradil notably on α_{1A} channels. We assessed whether this process could be evidenced in our experimental conditions. However, we found that increasing the frequency of stimulation from 0.1 Hz to 1 Hz strongly decreased the current generated by α_{1A} subunit expressed with β_{1b}. This decrease reflected spontaneous inactivation promoted by the stimulation rate which would indeed favor voltage-depend block as described in Fig. 3. By contrast, with β_{2a} instead of β_{1b}, a similar increase in the frequency of stimulation had no effect on α_{1A} currents. Therefore we used this subunit combination that minimized the contribution of spontaneous voltage-dependent block to explore the use-dependent inhibition. In agreement with the work of Bezprozvanny and Tsien (1995), we found that an increase in the stimulation rate strengthens the action of Mibefradil (Fig. 7B). Thus, we conclude that Mibefradil can block Ca^{2+} channels with several mechanisms.

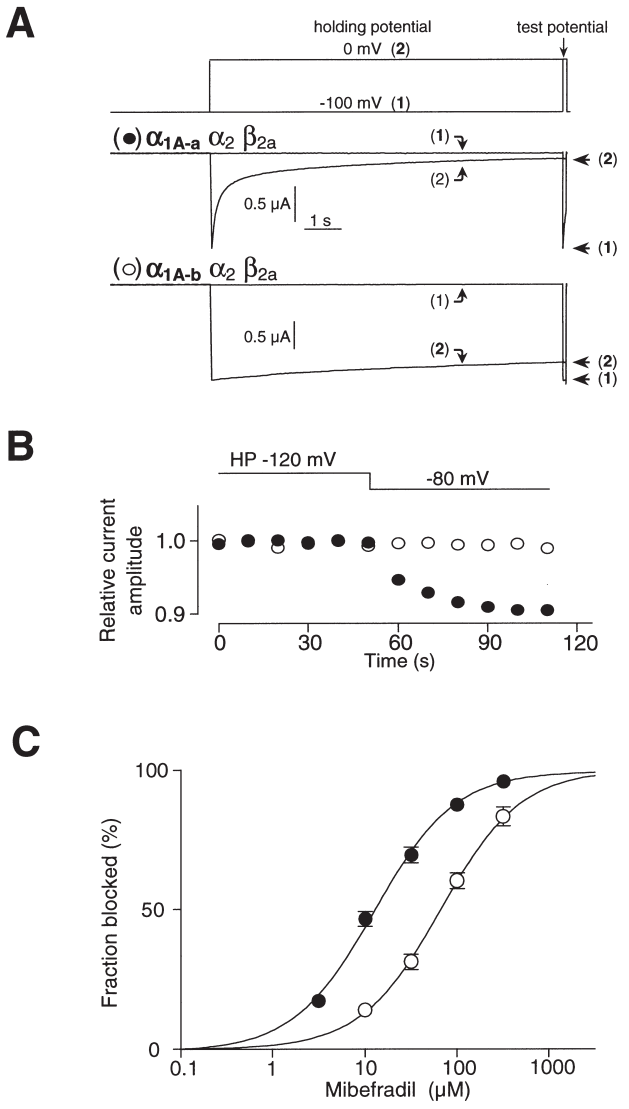

Fig. 6. Differential Mibefradil antagonism of α_{1A} splice variants expressed in *Xenopus* oocytes. (A) Differential inactivation properties of the two α_{1A} splice variants. Holding the potential to 0 mV for 15 s prior the test pulse almost totally inactivated current generated by the α_{1A-a} isoform while in contrast, the same protocol only produced a small reduction of the current supported by the α_{1A-b} isoform (by ~20%). (B) Fractional channel inactivation at −80mV under conditions closer to steady state as described by Bezprozvanny and Tsien (1995). Note that for α_{1A-b} the inactivated fraction is essentially zero while for α_{1A-a}, around 10% of the current is inactivated. (C) Dose-response of Mibefradil blockade of the α_{1A} isoforms. Note that the α_{1A-b} channels are less sensitive to the drug. Currents were evoked by 100ms step depolarizations from −80mV to 0mV delivered at 0.1 Hz.

4. Discussion

The repertoire of therapeutic molecules acting on VGCCs (also called Ca^{2+} channel antagonists) is to date restricted to L type channels, and therefore preferentially targets cell types expressing these channels (mostly cardiovascular cells). In contrast a recently developed molecule, Mibefradil, has been reported to be more selective for T-type vs L-type Ca^{2+} channels in cardiovascular tissues (Mishra and Hermsmeyer, 1994; Benardeau and Ertel, 1998). Therefore T-type Ca^{2+} channel blockade appeared to be the most straightforward molecular explanation of the drug's therapeutic benefit (Ertel et al., 1997). However this should be re-examined as, i) a clear role of T-channels in cardiovascular physiology has yet to be established; and ii) Mibefradil can also potently block most High-Voltage-Activated Ca^{2+} channel subtypes (Viana et al., 1997; Randall and Tsien, 1997; McDonough and Bean, 1998), including partially inactivated cardiac L-type channels (Mangoni et al., 1997). Thus the question as to whether the clinical effects of Mibefradil may involve a broader action on diverse Ca^{2+} channel subtypes should be addressed. The molecular mechanisms governing the interactions between Mibefradil and various types of recombinant Ca^{2+} channels expressed in mammalian were therefore dissected in detail.

4.1. α_{1A}, α_{1B} and α_{1C} currents at physiological calcium concentration

Our experiments provide the first comparison of the functional properties and Mibefradil sensitivity of α_{1A}, α_{1C} and α_{1E} channels expressed in mammalian cells at physiological external calcium concentration. Compared to *Xenopus* oocytes, the recipient cells mostly used so far to compare cloned Ca^{2+} channel properties, the kinetics of recombinant channels in tsA201 cells are more closely related to that of their native counterparts. As observed in oocytes (Bezprozvanny and Tsien, 1995), application of Mibefradil inhibited recombinant α_{1A}, α_{1C}, and α_{1E} channels with a one to one Ca^{2+} channel–Mibefradil interaction. The drug was clearly less effective on α_{1C} L-type Ca^{2+} channels than on α_{1A} and α_{1E}. In terms of specificity the inhibition by Mibefradil of both α_{1A} and α_{1E} channels coexpressed with β_{1b} was quite similar to that reported for native T-type Ca^{2+} channels or recombinant α_{1H} (Cribbs et al., 1998). In comparison to the oocyte expression system, we observed an increased potency of the drug and a larger difference in sensitivity between α_{1C}, and α_{1A} or α_{1E} (but see below the role of β subunit).

4.2. Voltage-dependent effects of Mibefradil

An important feature of Ca^{2+} channel antagonists is their mode of action on the channel itself (Hering et al., 1998). For example, DHPs have a better affinity at depolarized membrane potential for the inactivated state of L-type Ca^{2+} channels (Bean, 1984). Our results show that state-dependent block with Mibefradil is not restricted to L-type channels (α_{1C}), but is a common feature for all the α_1 subtypes, in agreement with Bezprozvanny and Tsien (1995). Analysis of our results using the

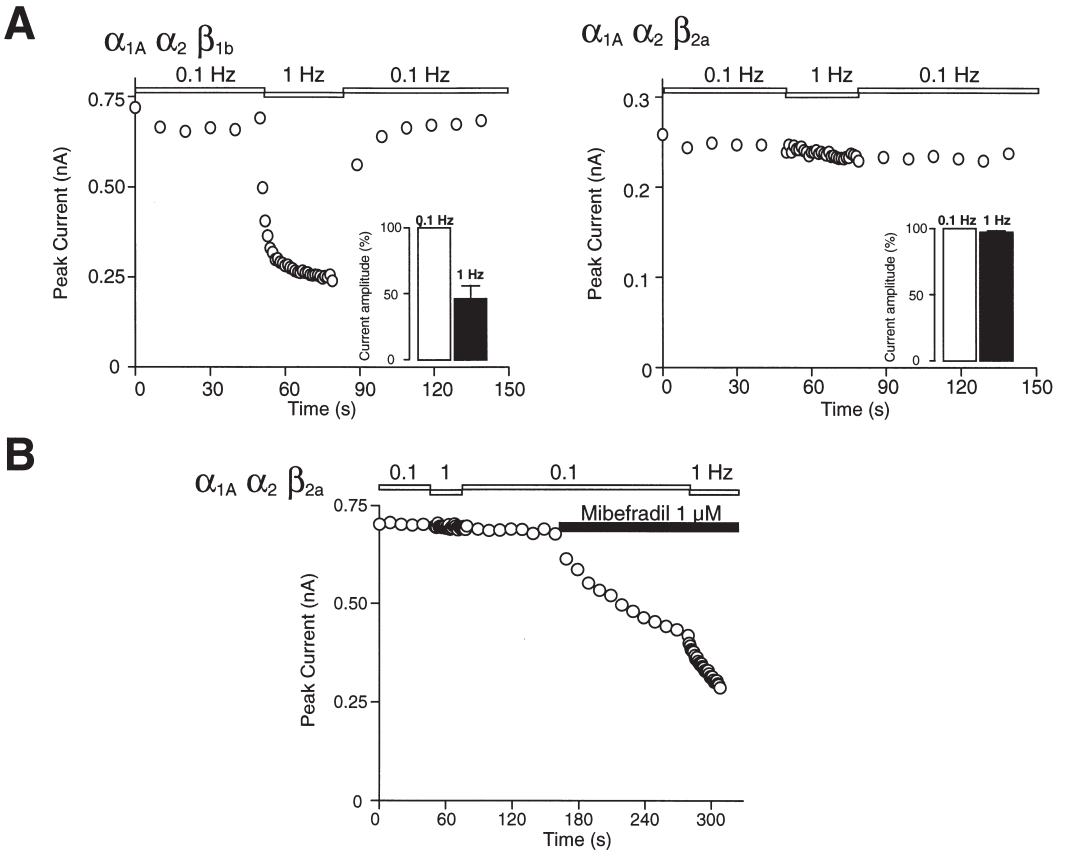

Fig. 7. Use-dependent block of α_{1A} Ca^{2+} channels by Mibefradil. (A) Effect of changing the frequency of stimulation from 0.1 Hz to 1 Hz on α_{1A} calcium currents. Note that this acceleration in the frequency profoundly reduced α_{1A} α_2 β_{1b} currents (left panel) while it spared α_{1A} α_2 β_{2a} currents (right panel). The histograms in insets are means of four to five experiments. (B) Acceleration of stimulation frequency enhanced α_{1A} (+α_2 β_{2a}) channel block by Mibefradil (1 μM). Depolarization of 50 ms in duration to 0 mV were applied from −100 mV every 10 s (0.1 Hz) or 1 s (1 Hz).

modulated receptor hypothesis (as in Bean, 1984; Bezprozvanny and Tsien, 1995; McDonough and Bean, 1998) showed that the affinity for the inactivated state is 50 to 100 fold higher than for the resting state (not shown). However, despite this homology with L-type channel block by DHPs, published studies using chimeras of α_{1C} and α_{1E} led to the conclusion that Mibefradil and DHP have distinct receptor sites (Schuster et al., 1996). Thus distinct drug binding sites on Ca^{2+} channels can support state-dependent block.

4.3. Factors affecting voltage-dependent inactivation modulate Mibefradil block

Various factors account for the wealth of heterogeneity in calcium channel inactivation, including the different combinatorial possibilities provided by the diverse α_1 and β subunits, and the existence of variants generated by alternative splicing within each class of subunit. However there has been essentially no report of altered pharmacology as a consequence of these factors. Our data supports a close control of the Mibefradil receptor site by factors governing voltage-dependent inactivation. First, coexpression of α1 subunits with β_{2a} markedly reduced the degree of Mibefradil block of channels subtypes exhibiting "pure" voltage-dependent inactivation. This occurred typically with α_{1A} and α_{1E}. In contrast, with α_{1C} channels which display weak voltage-dependent inactivation compared to prominent Ca^{2+}-dependent inactivation, the effect of β_{2a} coexpression on Mibefradil block is less pronounced. This suggests that the EF-hand region in the α_{1C} carboxy terminus which accounts for Ca^{2+}-sensitive inactivation (DeLeon et al., 1995) does not interfere with Mibefradil binding. Second, the ultra slow voltage-dependent inactivation of α_{1A} channels generated by a single Valine insertion in the intracellular loop between domains I and II, also reduced Mibefradil blocking affinity. Third, it is interesting to note that both β_{2a} coexpression and the Valine insert in the domain I–II linker of α_{1A} which are cumulative in terms of slowing inactivation, are also additive in terms of reducing the effects of Mibefradil. Therefore our results suggest that the blocking properties of Mibefradil closely depend on factors affecting voltage-dependent inactivation of Ca^{2+} channels. These include differences in the subunit composition of Ca^{2+} channels, but also many other factors

known to alter voltage-dependent inactivation properties such as channel-syntaxin interactions (Bezprozvanny et al., 1995) or the phosphorylation state of the channel (Stea et al., 1995).

4.4. Pharmacological implications

Consequently to understand the effect of Mibefradil and Ca^{2+} channel antagonists in general, it is crucial to consider both tissue and sub-cellular localization of calcium channel subunits as well as their specific associations. It has been demonstrated that Mibefradil does not cross the blood brain barrier and therefore has an effect limited to the cardiovascular system, inducing hypotension without increasing heart frequency.

It is well established that the ubiquitous and predominant Ca^{2+} channel in the different adult cardiovascular muscle cells is the L-type, with in some case coexistence with T-type. Thus, even if Mibefradil is more selective for T-type versus L-type channels, the effect of T-type channel inhibition in the hypotensive action of the drug remains obscure. So far, T-type Ca^{2+} channels have been identified in cultured but rarely in freshly dissociated arterial myocytes (Richard and Nargeot, 1998). In agreement with this finding, no evidence for a role of T-type Ca^{2+} channels in the contractile activity of smooth muscle cells has been provided. Therefore, blockade of the diverse vascular smooth muscle L-type Ca^{2+} channels is certainly a candidate mechanism to explain the hypotensive effect, considering the state-dependent block by Mibefradil and the depolarized resting potential of these cells. Moreover, at the molecular level, the α_{1C} gene is able to generate a splice variant giving rise to marked voltage-dependent inactivation and probably a more pronounced affinity for Mibefradil (Soldatov et al., 1997). The tissue distribution of these splice variants needs to be taken into account. In addition, another factor that might contribute to an increased Mibefradil sensitivity of L-type Ca^{2+} channels is the presence of the β_3 subunit isoform in human smooth muscle cells (Collin et al., 1994), since this isoform is the most efficient in conferring fast inactivation to nearly all $\alpha 1$ subunits (Olcese et al., 1994).

Apart from muscle cells, Mibefradil certainly blocks non L-type Ca^{2+} channels in neuronal and neuroendocrine cells within the cardiovascular system, such as the intracardiac and vascular parasympathetic and sympathetic nerve terminals and chromaffin cells. In these cell types, at synaptic endings in particular, neurotransmitter release is triggered by P/Q- and N-type channels (α_{1A} and α_{1B} subunits), and possibly R-type channels (α_{1E}, Jeons and Wurster, 1997). The potent inhibition of these channels by Mibefradil, and consequently the inhibition of neurohumoral control of vasculature may be involved in the overall effect of the drug. Consistent with this idea, a recent report showed that Mibefradil at clinical doses inhibits noradrenaline release in human heart though a blockade of N-type channels (Gothert and Molderings, 1997). Block of the sympathetic tone would also be expected to play a role on perivascular nerve endings, since the density of these synapses is increased in hypertensive animal models such as SHR rats (Burnstock, 1993).

5. Concluding remarks

Altogether, our data are consistent with a voltage-dependent block which implies that Ca^{2+} channel diversity resulting from combinations of the different types of $\alpha 1$ subunits (and their respective variants) and the different β subunits may significantly affect pharmacological properties. Demonstration of a potent block by Mibefradil of various HVA calcium channels in the same range of concentration as that blocking T-type channels should contribute to our understanding of the drug effects, and to further development of derivatives for new therapeutic targets, notably in the CNS.

Acknowledgements

We are grateful to Ed Perez Reyes for providing the β_{2a} cDNA and to Robert Koen for the Mibefradil. We thank Gerald Zamponi, Mike Seagar and Matteo Mangoni for careful reading of the manuscript. This work was supported by NATO grant CGR971546 (E.B.), by Ministerio de Educación y Cultura Español fellowship (C.J.), by AFM grant (J.N.), and by Produits Roche, Neuilly, France.

References

Aczél, S., Kurka, B., Hering, S., 1998. Mechanism of voltage- and use-dependent block of class A Ca^{2+} channels by Mibefradil. British Journal of Pharmacology 125, 447–454.

Bezprozvanny, I., Tsien, R.W., 1995. Voltage-dependent blockade of diverse types of voltage-gated Ca^{2+} channels expressed in *Xenopus* Oocytes by the Ca^{2+} channel antagonist Mibefradil (Ro 40-5967). Molecular Pharmacology 48, 540–549.

Bezprozvanny, I., Scheller, R.H., Tsien, R.W., 1995. Functional impact of syntaxin on gating of N-type and Q-type calcium channels. Nature 378, 623–626.

Bean, B.P., 1984. Nitrendipine block of cardiac calcium channels: high-affinity binding to the inactivated state. Proceedings of the National Academy of Sciences USA 81, 6388–6392.

Benardeau, A., Ertel, E.A., 1998. Selective block of myocardial T-type calcium channel by Mibefradil: a comparison with the 1,4-dihydropyridine Amlodipine. In: Tsien, R.W., Clozel, J.-P., Nargeot, J. (Eds.), Low-Voltage-Activated T-type Calcium channels. Adis International Limited, Chester, pp. 386–394.

Bourinet, E., Zamponi, G.W., Stea, A., Soong, T.W., Lewis, B.A., Jones, L.P., Yue, D.T., Snutch, T.P., 1996. The α_{1E} calcium chan-

nel exhibits permeation properties similar to low-voltage-activated calcium channels. Journal of Neuroscience 16 (16), 4983–4993.

Bourinet, E., Soong, T.W., Sutton, K., Slaymaker, S., Mathews, E., Monteil, A., Zamponi, G.W., Nargeot, J., Snutch, T.P., 1999. Splicing of α_{1A} subunit gene generates phenotypic variants of P- and Q-type calcium channels. Nature Neuroscience 2, 407–415.

Burnstock, G., 1993. Changing face of autonomic and sensory nerves in the circulation. In: Edvinsson, L., Uddman, R. (Eds.), Vascular innervation and receptor mechanisms: new perspectives. Academic Press Inc, San Diego, pp. 1–22.

Collin, T., Lory, P., Taviaux, S., Courtieu, C., Guilbault, P., Berta, P., Nargeot, J., 1994. Cloning, chromosomal location and functional expression of the human voltage-dependent calcium-channel beta 3 subunit. European Journal of Biochemistry 220, 257–262.

Cribbs, L.L., Lee, J.-H., Satin, J., Zhang, Y., Daud, A., Barclay, J., Williamson, M.P., Fox, M., Rees, M., Perez-Reyes, E., 1998. Cloning and characterization of α_{1H} from human heart, a member of the T-type Ca^{2+} channel gene family. Circulatory Research 83, 103–109.

DeLeon, M., Wang, Y., Jones, L., Perez-Reyes, E., Wei, X., Soong, T.W., Snutch, T.P., Yue, D.T., 1995. Essential Ca^{2+}-binding motif for Ca^{2+}-sensitive inactivation of L-type Ca^{2+} channels. Science 270, 1502–1506.

Ertel, S.I., Ertel, E.A., Clozel, J.P., 1997. T-type Ca^{2+} channels and pharmacological blockade: potential pathophysiological relevance. Cardiovascular Drugs Theory 11, 723–739.

Fisher, S.E., Ciccodicola, A., Tanaka, K., Curci, A., Desicato, S., D'Urso, M., Craig, I.W., 1997. Sequence-based exon prediction around the synaptophysin locus reveals a gene-rich area containing novel genes in human proximal Xp. Genomics 45, 340–347.

Gothert, M., Molderings, G.J., 1997. Mibefradil- and omega-conotoxin GVI-induced inhibition of noradrenaline release from the sympathetic nerves of the human heart. Naunyn Schmiedebergs Archives of Pharmacology 356 (6), 860–863.

Hering, S., Berjukow, S., Aczél, S., Timin, E.N., 1998. Ca^{2+} channel block and inactivation: common molecular determinants. Trends in Pharmacological Science 19, 439–443.

Jeons, S.-W., Wurster, R.D., 1997. Calcium channel currents in acutely dissociated intracardiac neurons from adult rats. Journal of Neurophysiology 77, 1769–1778.

Lee, J.-H., Daud, A.N., Cribbs, L.L., Lacerda, A.E., Pereverzev, A., Klöckner, U., Schneider, T., Perez-Reyes, E., 1999. Cloning and expression of a novel member of the low voltage-activated T-type calcium channel family. Journal of Neuroscience 19, 1912–1921.

Mangoni, M.E., Leuranguer, V., Bourinet, E., Richard, S., Nargeot, J., 1997. Block of cardiac Ca^{2+} channels by the new Ca^{2+} antagonist Ro 40-5967: Consequence on heart rate and cardiac output. Biophysics Journal 72, A256.

McDonough, S.I., Bean, B.P., 1998. Mibefradil inhibition of T-type calcium channels in cerebellar Purkinje neurons. Molecular Pharmacology 54, 1080–1087.

Mishra, S.K., Hermsmeyer, K., 1994. Selective inhibition of T-type Ca^{2+} channels by Ro 40-5967. Circulatory Research 75, 144–148.

Olcese, R., Qin, N., Schneider, T., Neely, A., Wei, X., Stefani, E., Birnbaumer, L., 1994. The amino terminus of a calcium channel beta subunit sets rates of channel inactivation independently of the subunit's effect on activation. Neuron 13 (6), 1433–1438.

Parent, L., Gopalakrishnan, M., Lacerda, A.E., Wei, X., Perez-Reyes, E., 1995. Voltage-dependent inactivation in a cardiac-skeletal chimeric calcium channel. FEBS Letters 360, 144–150.

Perez-Reyes, E., Cribbs, L.L., Daud, A., Lacerda, A.E., Barclay, J., Williamson, M.P., Fox, M., Rees, M., Lee, J.-H., 1998. Molecular characterization of a neuronal low-voltage-activated T-type calcium channel. Nature 391, 896–900.

Qin, N., Platano, D., Olcese, R., Costantin, J.L., Stefani, E., Birnbaumer, L., 1998. Unique regulatory properties of the type 2a Ca^{2+} channel β subunit caused by palmitoylation. Proceedings of the National Academy of Sciences USA 95, 4690–4695.

Randall, A.D., Tsien, R.W., 1997. Contrasting biophysical and pharmacological properties of T-type and R-type calcium channels. Neuropharmacology 36 (7), 879–893.

Richard, S., Nargeot, J., 1998. T-type calcium currents in vascular smooth muscle cells: a role in cellular proliferation? In: Tsien, R.W., Clozel, J.-P., Nargeot, J. (Eds.), Low-Voltage-Activated T-type Calcium channels. Adis International Limited, Chester, pp. 123–132.

Schuster, A., Lacinova, L., Klugbauer, N., Ito, H., Birnbaumer, L., Hofmann, F., 1996. The IVS6 segment of the L-type calcium channel is critical for the action of dihydropyridines and phenylalkylamines. EMBO Journal 15 (10), 2365–2370.

Soldatov, N.M., Zuhlke, R.D., Bouron, A., Reuter, H., 1997. Molecular structures involved in L-type calcium channel inactivation. Role of the carboxyl-terminal region encoded by exons 40-42 in alpha1C subunit in the kinetics and Ca^{2+} dependence of inactivation. Journal of Biological Chemistry 272 (6), 3560–3566.

Soong, T.W., Stea, A., Hodson, C.D., Dubel, S.J., Vincent, S.R., Snutch, T.P., 1993. Structure and functional expression of a member of the low voltage-activated calcium channel family. Science 260, 1133–1136.

Stea, A., Tomlinson, J.W., Soong, T.W., Bourinet, E., Dubel, S.J., Vincent, S.R., Snutch, T.P., 1994. The localization and functional properties of a rat brain α_{1A} calcium channel reflect similarities to neuronal Q- and P-type channels. Proceedings of the National Academy of Sciences USA 91, 10576–10580.

Stea, A., Soong, T.W., Snutch, T.P., 1995. Determinants of PKC-dependent modulation of a family of neuronal calcium channels. Neuron 15, 926–940.

Tomlinson, J.W., Stea, A., Bourinet, E., Charnet, P., Nargeot, J., Snutch, T.P., 1993. Functional properties of a neuronal class C L-type calcium channel. Neuropharmacology 32, 1117–1126.

Viana, F., Van den Bosch, L., Missiaen, L., Vandenberghe, W., Droogmans, G., Nilius, B., Robberecht, W., 1997. Mibefradil (Ro 40-5967) blocks multiple types of voltage-gated calcium channels in cultured rat spinal motoneurones. Cell Calcium 22 (4), 299–311.

Zhang, J.-F., Ellinor, P.T., Aldrich, R.W., Tsien, R.W., 1994. Molecular determinants of voltage-dependent inactivation in calcium channels. Nature 372, 97–100.